TITLE: Relating neuromuscular control to functional anatomy of limb muscles in extant archosaurs

AUTHORS: Cuff, A R; Daley, M A; Michel, K B; Allen, V R; Lamas, L P; Adami, C; Monticelli, P; Pelligand, L; Hutchinson, J R

JOURNAL: Journal of Morphology

PUBLISHER: Wiley

PUBLICATION DATE: 8 March 2019 (online)

DOI: https://doi.org/10.1002/jmor.20973

Relating neuromuscular control to functional anatomy of limb muscles in extant archosaurs

Short title: Archosaur EMG patterns

Andrew R. Cuff[1], Monica A. Daley[1], Krijn B. Michel[1], Vivian R. Allen[1], Luis Pardon Lamas[1,2], Chiara Adami[3], Paolo Monticelli[3], Ludo Pelligand[3], John R. Hutchinson[1]

[1] Structure and Motion Laboratory, Department of Comparative Biomedical Sciences, Royal Veterinary College, Hawkshead Lane, North Mymms, Hertfordshire, AL9 7TA, United Kingdom.

[2] Current address: Faculdade de Medicina Veterinária, Universidade de Lisboa, Pólo 7, Universitário da Ajuda, 1300-477, Lisboa, Portugal.

[3] Queen Mother Hospital, Department of Clinical Science and Services, Royal Veterinary College, Hawkshead Lane, North Mymms, Hertfordshire, AL9 7TA, United Kingdom.

Abstract

Electromyography (EMG) is used to understand muscle activity patterns in animals. Understanding how much variation exists in muscle activity patterns in homologous muscles across animal clades during similar behaviours is important for evaluating the evolution of muscle functions and neuromuscular control. We compared muscle activity across a range of archosaurian species and appendicular muscles, including how these EMG patterns varied across ontogeny and phylogeny, to reconstruct the evolutionary history of archosaurian muscle activation during locomotion. EMG electrodes were implanted into the muscles of turkeys, pheasants, quail, guineafowl, emus (three age classes), tinamous and juvenile Nile crocodiles across 13 different appendicular muscles. Subjects walked and ran at a range of speeds both overground and on treadmills during EMG recordings. Anatomically similar muscles such as the lateral gastrocnemius exhibited similar EMG patterns at similar relative speeds across all birds. In the crocodiles, the EMG signals closely matched previously published data for alligators. The timing of lateral gastrocnemius activation was relatively later within a stride cycle for crocodiles compared to birds. This difference may relate to the coordinated knee extension and ankle plantarflexion timing across the swing-stance transition in Crocodylia, unlike in birds where there is knee flexion and ankle dorsiflexion across swing-stance. No significant effects were found across the species for ontogeny, or between treadmill and overground

locomotion. Our findings strengthen the inference that some muscle EMG patterns remained conservative throughout Archosauria: for example, digital flexors retained similar stance phase activity and M. pectoralis remained an “anti-gravity” muscle. However, some avian hindlimb muscles evolved divergent activations in tandem with morphofunctional changes such as bipedalism and more crouched postures, especially M. iliotrochantericus caudalis switching from swing to stance phase activity and M. iliofibularis adding a novel stance phase burst of activity.

Keywords: morphology, neural control, musculoskeletal system, evolution, locomotion.

Research Highlights

Crocodilians show appendicular muscle activity patterns linked to ancestral conservatism. Birds show consistent differences from the ancestral state, which may have been inherited from dinosaurian ancestors after the Triassic archosaurian divergence.

Introduction

Animals move using coordinated patterns of muscular activity stimulated by motor neurons. The electrical signals associated with neuromuscular excitation and thence activation can be obtained using electromyography (EMG). The relative amplitudes and timings of EMG signals can be used to (qualitatively) approximate muscle force (Roberts and Gabaldón, 2008). Integrating EMG with kinematic data and anatomical information facilitates interpretation of the individual function of muscles (e.g. Roberts and Gabaldón, 2008; Carr et al., 2011).

Collecting EMG from non-human animals is difficult because surface EMG require ideal conditions (thin skin, minimal skin motion, clean attachment sites, conductive gels, good adhesion, etc.) which are not readily achieved in many animals. As such, the majority of EMG data in animals have been collected by surgically implanted electrodes. Probably because of the difficulties inherent in

collecting EMG data from appendicular muscles during locomotion and ethical priorities to minimize the number of invasive animal experiments, only a small range of non-mammalian amniote taxa (and muscles) have been studied. These studies include birds (Jacobson and Hollyday, 1982; Gatesy, 1994, 1999; Daley and Biewener, 2003, 2011; Marsh et al., 2004; Daley et al., 2009; Ellerby and Marsh, 2010; Gordon et al., 2015), but also alligators (Gatesy, 1991, 1994, 1997; Reilly et al., 2005), caiman (Gatesy, 1994), turtles (Rivera et al., 2011; Rivera and Blob, 2013), and lizards (Jenkins and Goslow, 1983; Reilly, 1995; Higham and Jayne, 2004; Foster and Higham, 2014, 2017). The majority of these works have focussed on using these species as models for specific mechanistic questions. However, a few studies have attempted to understand muscle activation patterns with the explicit goal of reconstructing the evolutionary diversification of limb motor function (Gatesy and Dial, 1993, 1996; Gatesy, 1994, 1999; Rivera and Blob, 2013).

Better understanding of the relationships between morphology and muscle activity will enable prediction of function for animals (whether extant or extinct) for which no data exist. Such predictions are particularly important for lineages characterized by major changes in functional disparity, such as the Archosauria (“ruling reptiles”; Crocodylia, birds/Aves, and all descendants of their most recent common ancestor). For such clades there is a need to better predict function from form. Archosauria is a clade that diversified first during Triassic period ~250 Mya, evolving a wide variety of forms including small- and large-bodied, sprawling/erect-limbed, quadrupedal/bipedal, aquatic/amphibious/terrestrial and flightless/flying. EMG data from extant archosaurs, particularly the timings of activation during the stride cycle, have been used to infer locomotor changes across Archosauria as a whole (Gatesy, 1994, 1999; Gatesy and Dial, 1996; Hutchinson and Gatesy, 2000). The taxonomic sampling of these EMG data remains somewhat sparse, prompting the question of whether variation in EMG patterns within extant Crocodylia or Aves might alter inferences of neuromotor evolution in Archosauria.

Available hindlimb EMG data for birds are largely restricted to guineafowl (e.g. Gatesy, 1999; Marsh et al., 2004; Higham et al., 2008; Daley et al., 2009; Ellerby and Marsh, 2010; Carr et al., 2011; Daley and Biewener, 2011; Gordon et al., 2015) and domestic chickens (e.g. Jacobson and Hollyday, 1982; Bradley and Bekoff, 1992), although some data exist for wild turkeys (Roberts and Gabaldón, 2008), mallard ducks (*Anas platyrhynchos*) (Biewener and Corning, 2001) and pigeons (Gatesy and Dial, 1993, 1996). These data have revealed some consistent patterns of muscle activity such as co-activation of muscle pairs (e.g. M. flexor cruris lateralis pars pelvica (hip extension and knee flexion) and M. gastrocnemius pars lateralis (knee flexion and ankle extension) (Ellerby and Marsh, 2010). Almost all avian taxa for which hindlimb EMG data currently exist belong to the clade Galliformes (except mallard ducks – Anseriformes; and pigeons – Columbiformes), a useful model system because they are relatively terrestrial and athletic compared to many other species belonging to the speciose avian clade Neognathae. Hence, almost all present understanding of neuromuscular control of hindlimb function in crown-clade Aves is based upon the assumption that Galliformes represents the typical pattern for all or most birds. This assumption seems reasonable, but it deserves further testing with more data from some of the 9000+ species of extant Aves.

Importantly, there have been no hindlimb EMG studies of the sister group of Neognathae, the Palaeognathae. The palaeognaths include highly specialized, terrestrial, long-limbed (cursorial) forms such as ostriches, emus, rheas, cassowaries and kiwis, but also the tinamous. Tinamous are of particular interest because they are more similar to “ancestral avian” morphology compared to other paleognaths, with small body size and retained flight capability, and are perhaps even more plesiomorphic in locomotor function than many galliforms (Yonezawa et al., 2017). Prior studies have simulated hindlimb muscle activities in larger palaeognaths (emus (Goetz et al., 2008) and ostriches (Rankin et al., 2016)), which would benefit from further data for experimental validation.

Here, we present hindlimb EMG data during walking and running from two palaeognath species (elegant-crested tinamous - *Eudromia elegans*, and emus - *Dromaius novaehollandiae*), and four galliform species (helmeted guineafowl - *Numida meleagris*, wild American turkey - *Meleagris gallopavo,* common pheasant – *Phasianus colchicus* and bobwhite quail - *Colinus virginianus*). We aim to test whether morphologically conserved hindlimb muscles function similarly across a broad range of Aves indicated by activation during the same phases of the stride cycles at similar speeds.

Birds span the range of ontogenetic strategies from altricial to precocial, with precocial birds appearing to be miniatures of their adult form. In chickens (precocial), the neural pathways that drive locomotion appear to arise before hatching, enabling them to walk within hours of hatching (Bekoff, 1976; Bekoff et al., 1987; Bradley et al., 2014). There may also be developmental changes in neural control and muscle activity within birds as they grow (e.g. Tobalske et al., 2017), similar to that seen in certain turtle species (Blob et al., 2008). We measured ontogenetic variation of post-hatching neuromuscular control within emus from young birds (< 4kg) to adults (>30kg), for comparison with existing data on ontogenetic scaling of limb muscles (Lamas et al., 2014) and ontogenetic changes of EMG patterns in chickens post-hatching (Bekoff, 1976; Bekoff et al., 1987; Bradley et al., 2014).

Finally, we broaden our study's perspective to cover extant Archosauria by including novel EMG data from Nile crocodiles (*Crocodylus niloticus*). Similarly to birds, all knowledge of appendicular neuromuscular control in Crocodylia is based on the less diverse subclade Alligatoroidea (Gatesy, 1991, 1994, 1997; Reilly et al., 2005); almost exclusively *Alligator mississippiensis*. By adding EMG measurements from a representative taxon within the more diverse clade Crocodyloidea, we will test if similar EMG patterns hold for Crocodylia as a whole, or even more broadly within Archosauria, Sauria or Tetrapoda (*vide* Gatesy, 1994, 1999). Furthermore, work on birds (domestic chickens)

129 comparing overground and treadmill locomotion show minor differences in EMG patterns (Jacobson
130 and Hollyday, 1982), so we test whether this is the case in crocodilians too.

131

132 Overall, we aim to use this extensive dataset on muscle activity patterns to revisit the questions
133 raised by Gatesy (1994, 1999) about how much diversity exists in the neuromuscular control of
134 locomotion among archosaurs. This comparative dataset will have intrinsic value in applications to
135 other archosaurs; both extant and extinct (e.g. Hutchinson and Gatesy, 2000; Rankin et al., 2016).

136

137 **Methods**

138 All species, numbers of individuals used, ontogenetic stage, sexes and body masses are listed in
139 Table 1.

140 Ethics

141 EMG data collection with Nile crocodiles and Elegant-crested tinamous, and the guineafowl and
142 pheasant procedures, were conducted at the RVC Structure and Motion Laboratory under two
143 different project licences approved by the college's Ethics and Welfare committee and granted by
144 the Home Office (United Kingdom). Bobwhite quail and wild turkey data were collected at the
145 Concord Field Station of Harvard University, following procedures licensed and approved by the
146 Harvard Institutional Animal Care and Use Committee in accordance with the guidelines of the
147 National Institutes of Health and the regulations of the United States Department of Agriculture.

148 Surgical procedures

149 For all species bipolar EMG electrodes were constructed of two strands of 0.004 inch diameter
150 platinum pure TC grade (100896) insulated by heavy poly-nylon (HPN) (California Fine Wire
151 Company, CA, USA) soldered to a connector. The free ends of the electrodes had a staggered 1mm

exposed wire region spaced 1.5mm apart. The electrodes were implanted under surgical anaesthesia appropriate for that species (see details below). Surgeries involved: 1) making skin incisions over the locations of electrode placement, 2) intramuscular implantation of fine-wire bipolar electrodes, 3) subcutaneous tunnelling of electrodes to a connector on the dorsum or proximal hindlimb, 4) closure of incisions and 5) peri- and post-operative administration of analgesia. The recorded muscles (and their in-text abbreviations) are in Tables 2 and 3.

Emu

Six emus were anaesthetised either using mask inhalation of 5% isoflurane for the chicks, or using intramuscular injections of xylazine (3mg/kg) and ketamine (15mg/kg) to the left caudolateral shank muscles for the juveniles and adults. After inductions, the birds were intubated with an endotracheal tube and maintained at an adequate surgical anaesthetic plane with a variable concentration of inhaled isoflurane. Breathing, heart rate and body temperature were monitored throughout surgery. The feathers in the surgical field were clipped and incisions were made for electrode implantation. The EMG electrodes were successfully implanted into M. Iliotrochantericus caudalis (ITC), M. iliotibialis lateralis pars postacetabularis (ILPO), M. iliofibularis (ILFB) and M. gastrocnemialis pars lateralis (GL) (Figure 1). All wires exited via a skin incision caudal to the femoral trochanteric crest of the right pelvic limb. After surgery, animals were rested in their habitual pen and administered non-steroidal anti-inflammatories (meloxicam 1.5mg/kg, three times a day) until data collection was completed. Birds were assessed for discomfort before and throughout data collection; which started 24 hours post-surgery; studies were postponed or interrupted if the animals appeared distressed or lame.

Other birds

The guineafowl, pheasant, quail and turkey all underwent surgical procedures that have been described previously (Daley and Biewener, 2003, 2011; Daley et al., 2009), with the birds anaesthetised using isoflurane delivered via a mask. The tinamous followed a similar method (see supplementary information for a more detailed protocol), although general anaesthesia was induced using intramuscular injection of 0.075 mg/kg Ketamine (Ketamidor, Chanelle UK) and 22mg/kg medetomidine (Sedastart, Animalcare UK) into the right pectoral muscle, and maintained using inhaled sevoflurane using a non-cuffed endotracheal tube throughout the remainder of the procedure. The surgical field was plucked of feathers and sterilised, and incisions were made over the target muscles. The EMG electrodes were then implanted into the target muscles, while connected to a micro-connector placed on the bird's back. The electrode leads were passed subcutaneously from a 1-2cm incision over the synsacrum to the larger primary incision (4-5cm) over the right lateral shank. Bipolar electrodes were constructed of 0.1mm diameter silver fine-wire (California Fine Wire, Inc., Grover Beach, USA) with 0.5-1.0mm bared tips, and 5-8mm spacing. Electrodes were emplaced using a 23 gauge hypodermic needle, and secured to the muscle using 5-0 silk suture; then skin incisions were closed using 3-0 silk. The birds were given analgesia every 12 hours and antibiotics every 24 hours. Experimental recordings took place over the next 1–3 days for most birds, but the tinamous were given six days to recover due to their potential sensitivity to stress (pers. obs.,) perhaps due to their relatively small hearts (Altimiras et al., 2017).

For all birds, the M. gastrocnemius pars lateralis (GL) was successfully implanted. Additionally, the M. flexor perforatus digiti IV (DFIV) was implanted in both the guineafowl and turkey. Some birds also had implantations into uniquely measured muscles: in the turkey M. flexor cruris lateralis pars pelvica (FCLP), in the guineafowl M. femorotibialis lateralis (FMTL) and in tinamous M. fibularis longus (FL). The basic anatomical positions of all of these muscles are shown in Figure 1, and their approximate actions listed in Table 2.

Nile Crocodiles

The anaesthetic procedure is covered in detail in Monticelli et al., (2019), but is briefly outlined here. General anaesthesia was induced using a combination of medetomidine (Sedastart, Animalcare Ltd., York, UK; 0.2 mg kg^{-1}) and ketamine (Ketamidor, Chanelle, Berkshire, UK; 10 mg kg^{-1}) intramuscularly in the left triceps brachii muscle. After anaesthetic induction, the crocodiles were intubated using an uncuffed endotracheal tube and anaesthesia was maintained using sevoflurane (SevoFlo, Zoetis, Belgium) in oxygen. Intramuscular meloxicam (Metacam, Boehringer Ingelheim, DE; 0.2 mg/kg) was administered in the perioperative period. Active warming was provided by either HotDog® (Augustine Surgical, Eden Prairie, MN, USA) or Bair Hugger® (3M, Maplewood, MN, USA) systems.

Five incisions, 1-2cm long, were made over the right ilium, proximolateral aspect of the tail, cranial thigh, and caudal and cranial aspects of the lateral shank to enable visualisation and intramuscular implantation for the four hindlimb implants. A further six incisions were made to access four forelimb muscles, with incisions at the scapula, cranial and caudal aspects of the upper arm, medial aspect of the lower arm, lateral aspect of the thorax, and ventral aspect of the thorax. Through these incisions, the muscles were implanted. After post-mortem, the muscles from which data were collected were confirmed to be M. transversus perinei (TP), M. iliotibialis 2 (IT2), M. gastrocnemius externus (GE), M. flexor digitorum longus (FDL) of the hindlimb and M. pectoralis (PEC) of the forelimb (Figure 1, Table 3).

The EMG electrode connector was anchored by suturing to two scutes near the dorsal-most incision (iliac or scapular). Each pair of electrode wires was then subcutaneously tunnelled to their respective insertion sites. Tunnelling was achieved subcutaneously using a section of size 3 (internal diameter)

uncuffed PVC endotracheal tubing and a looped guide wire. The electrodes were implanted using the sew-through method and secured with two simple-interrupted sutures using 3-0 vicryl to prevent both translation and rotation of the wires post-surgery. The excess wiring was pulled back through to the dorsal incisions where it was coiled and tucked back into the incision site. Each incision was then flushed with lidocaine and then closed using everted mattress stitches to prevent wound contamination in the water within the enclosures. The anaesthesia was discontinued and atipamezole (1 mg kg^{-1}) (Sedastop, Animalcare, UK) was administered intramuscularly in the left M. triceps brachii, and repeated after 30 minutes in case of residual sedation. The crocodiles were then given at least two days to recover in their enclosures before any data were collected

Experimental protocol

The tinamous were placed on a Starkerhund treadmill (Terraglione di Vigodarzere, Italy) within a box with transparent acrylic sides to allow visualisation of the footfalls, and which had an opening for the EMG wires. Trials ranged from 30s to 60s, with at least a 60s break between trials. The treadmill speed varied from 0.1ms^{-1} to 0.45ms^{-1}; faster speeds were not safely achievable with the birds. The trials were initiated using a trigger system that created a short light flash that could be seen by the two Hero 3+ GoPro cameras (San Mateo, CA, USA) recording at 60Hz which were used to capture the footfall patterns of the animals during locomotion. Trials were maximally 60s long, although usually far shorter, with at least 60s recovery between trials. The birds were in the experimental area for a maximum of 1hr before being returned to their enclosure. A total of 64 trials were collected for the two individuals, with the resulting data summarised in Table 5.

Emu experimental trials were conducted overground in a corridor of ~90cm width enclosed by wire netting for the younger individuals, and metal fencing for the adults. Due to the wired EMG implants, cable length limited the maximum length of the runway. Cable length was ~5m for the youngest birds and 9m for the two older groups. All wires were tethered along a sliding pulley system (suspended >1m off the ground) which kept the implant cables from dragging on the floor and interfering with gait. The floor of the runway was instrumented with eight Kistler forceplates (0.6x0.9m; model 9287B, Hook, Hampshire, UK), which were used to obtain timings of footfalls. The emus were also marked with polystyrene hemispheres covered with infrared-reflective tape (Scotchlite 8850; 3M, Manchester, UK) (1cm diameter for the youngest, 2cm diameter for the older individuals) for joint motion analysis for another study (Lamas, 2015), which included two dorsal midline body markers used here for obtaining locomotor velocities via a Qualisys Oqus 500 six-camera system recording at 250Hz (Qualisys AB, Göteborg, Sweden). Across the six individuals, 405 trials were completed, and the resulting trials are listed in Table 6.

The turkey (2 individuals, 5 trials), quail (2 individuals, 6 trials), guineafowl (2 individuals, 6 trials), and pheasant (1 individual, 1 trial) all ran on a custom-built treadmill, with a slatted black rubber-coated steel belt with a 55.8×172.7 cm running surface. The treadmill speeds were selected to achieve an approximately similar dimensionless speed (see below) of 1.25 across species (Table 5). Dimensionless speed is the square root of the Froude number (Alexander and Jayes, 1983):

$$u = \frac{v}{\sqrt{(g \cdot l)}}$$

where u is dimensionless speed, v is velocity (ms^{-1}), g is acceleration due to gravity ($9.81 ms^{-2}$) and l is standing (or mid-stance) hip height (in metres). Dimensionless speed usually assumes geometric similarity (Alexander and Jayes, 1983); however, dimensionless speed holds reasonably well across animals that use similar locomotor modes even if not strictly geometrically similar (see Daley and

Birn-Jeffery, 2018) and references therein for a thorough review). The turkey, quail and quineafowl were recorded using a Photron camera (Photron Europe Ltd., West Wycombe, UK) at 125Hz, whilst the pheasant was recorded using Qualisys cameras (as per the emus above) at 125Hz.

The crocodiles were captured from their enclosures and their mouths were taped to prevent injury to themselves or handlers, or damaging their EMG wires. The crocodiles were then either placed on a Starkerhund treadmill (within an acrylic-sided enclosure to prevent the animals escaping), or on a custom-made wooden runway (0.38x0.40x2.44m). Both the treadmill enclosure and custom wooden runway had openings in the roof to allow the wires to exit to be connected to the EMG amplifiers. The crocodiles were motivated to walk by stimulating the tail with a broom as needed. The hardware otherwise was the same as that used with the tinamou. Trials were maximally 60s long, although usually far shorter, with at least 60s recovery between trials. Across four individuals, a total of 160 trials were collected, with details of collected data in Table 4.

EMG recordings

Each of the sockets on the animals was connected via lightweight shielded cables to GRASS pre-amplifiers (P511, Natus Neurology Inc., Pleasanton, CA, USA). EMG signals remained at a constant amplification throughout data collection with a low-pass (10Hz for most birds; 30Hz for emus, tinamous and crocodiles) and a high-pass (10kHz) filter. The EMG signals were sampled at 2500Hz (emu) or 5000Hz (all other species). Signals were amplified between 1000 and 10000 times, but this varied between and within data collection sessions and individuals as required to obtain visible signals.

Data processing

Footfall events (foot on and off times) were manually recorded from the videos for the crocodiles, tinamous, guineafowl, quail, turkey and pheasant for each trial. The emu footfall timing pattern was determined by analysing the forceplate data, with foot on and off timings linked to the force traces (recorded at 1000Hz; automatically filtered using a low-pass filter at 100Hz; threshold for foot on/off events = 1 % body weight). Custom scripts in Matlab software (MathWorks, Natick, MA, USA) were used for all post-processing.

The tinamous and crocodiles on the treadmill moved at three different speeds, the lowest being driven by an electric drill turning the drive wheel, the other two (approximately 0.5, 0.7mph) driven by the treadmill motor. The belt speed was calibrated from a video based on the movement of a mark on the treadmill belt relative to a point at a known distance on the treadmill frame. For the crocodiles on the runway, locomotor speed was measured by tracking the shoulder scutes (which had the least lateral movement relative to direction of movement) across 20cm, using a dorsally placed camera atop the runway. Emu speeds were calculated by tracking the cranial dorsal body marker in 3D space, then extracting the horizontal displacements and dividing by the time elapsed.

Data were then cut into individual steps based on footfall timings extracted from video or forceplate data from each species, described above. Each EMG sequence was filtered and then rectified. The data were bandpass-filtered with a low-pass cutoff between 50-90 Hz and a 12-order Butterworth filter applied, although the emu data underwent a 0.5 Hz low-pass filter to remove an underlying noise waveform before being filtered as the other data (see Figure 2 for representative filtered EMG signals).

In species with multiple speeds, dimensionless speed was used for comparisons. As the emu trials spanned the largest range of dimensionless speeds, they were grouped into 0.2*u* bins from 0.3-1.5*u*. These bins covered all of the ontogenetic stages of the emu and overlapped with the recorded speed range of other studied bird species except for the tinamou, which never reached a dimensionless speed greater than 0.3. The crocodiles' speeds were also normalised to dimensionless speed where *l* is total hindlimb length instead of hip height due to the variety of postures (from sprawling to upright) that they used. For each species, the rectified sequences for each grouping (Table 2,3) were scaled to the same length with "foot-on" being 0 and 100 (equivalent to a full stride). The average and 95% confidence intervals for each of these groupings were then calculated using custom Matlab code. EMG onset was deemed to be where there were peaks beyond 10% of the baseline.

For one muscle (M. gastrocnemius lateralis/externus; GL/GE) there were sufficient data for statistical tests of gross similarity of EMG signals across Aves and Crocodylia. An inter-species cross-correlation analysis was carried out upon the average rectified EMG sequences for comparable speeds of 1.1-1.3*u* (or maximum speeds for tinamous and crocodiles), using custom Matlab scripts. Due to the small sample sizes in terms of both numbers of individuals and number of trials, no additional statistics were carried out.

Results

Birds

<u>Emus</u>

There were no major differences between the age groups in terms of muscle activation timings within the stride cycles. However, the baby emus may have had a slightly broader range of

activations for each muscle group relative to the older individuals. With so few individuals, it is difficult to resolve whether this difference related to individual variance or age (Figure 3).

ITC (Figure 3, S1)

The M. iliotrochantericus caudalis was active from late swing through to mid-stance . However, at slower relative speeds (below 1.1*u*), the late swing and early stance activations were at lower levels, and the peak activation occurred during mid-stance. At the fastest speeds, the activation peaked in early stance.

ILPO (Figure 3, S2)

The M. iliotibialis lateralis pars postacetabularis had variable activation with speed. At slower speeds (<0.7 *u*), the EMG signals occurred at a fairly consistent level of activity from the end of swing through late-middle stance phase. At faster relative speeds (0.7-0.9 *u*), the EMG signal peaked during mid-stance, with lower activity around late swing and later stance. At the fastest speeds (0.9-1.1 and 1.1-1.3 *u*), there was a discontinuity between the signal in late swing and the large peak at mid-stance; consistent with two bursts of activity.

ILFB (Figure 3, S3)

The M. iliofibularis displayed peak activation during early stance, but with activity persisting from late swing to mid-stance.

GL (Figure 3, S4)

The M. gastrocnemius pars lateralis of emus, like the ITC and ILFB, was active from late swing through mid-stance phase at most speeds. In the youngest emus, EMG activity extended through stance and into early swing at *u* from 0.3-0.5. At higher values of *u*, the initial muscle activations for all ages became increasingly earlier, so activation occurred more consistently during late swing and ended earlier in stance, with higher relative activations and a smaller range as a proportion of total stride time.

Tinamous (Figure 4, S5)

GL

Overall, the M. gastrocnemius pars lateralis EMG signals were similar across the small range in speeds, with activity beginning in late swing and continuing through early stance phase, with a reduced mid-late stance signal at faster speeds.

FL

From the one trial of 7 strides at 0.1ms^{-1} (0.06*u* - a very slow walk), the M. fibularis longus showed low level EMG activity from foot on through to late-middle stance phase.

Galliform birds

FCLP

The M. flexor cruris lateralis pars pelvica was only measured in turkeys, and was active through stance phase, with a peak in mid-stance (Figure 5, S6).

386 *FMTL*

387 The M. femorotibialis lateralis was only measured in the guineafowl, and was active from late swing
388 through to late stance phase (Figure 6, S7).

389

390 *GL*

391 Across the quail, pheasants, guineafowl and turkey, the lateral gastrocnemius showed a similar
392 overall pattern of activity, with the primary burst of muscle activity occurring from late swing to
393 early mid-stance phase, with peak activity early in stance (Figure 7A-D, S8).

394

395 *DFIV*

396 The M. flexor perforatus digiti IV was measured in turkeys and guineafowl, and showed similar
397 activity from late swing through early stance phase; as in the GL (Figures 5-6, S6-S7).

398

399

400 **Crocodiles** (Figure 8, S9)

401 *PEC*

402 The M. pectoralis for the Nile crocodiles showed low-level activation through mid-stance phase, with
403 maximal activation in late stance. Unlike the TP (below), the pattern was not shifted earlier in the
404 cycle at faster speeds; instead, there was relatively shorter period of activation. For relatively similar
405 speeds, there was no apparent difference between EMG signals for animals on treadmill or runways.

406

407 *TP*

The M. transversus perinei was active through early to mid-stance phase, with peak activity from 20-50% of the stride cycle. At faster speeds, the TP became active earlier, including late swing phase (Figure 8).

IT2

The M. iliotibialis 2 was active throughout most of the stance phase, with the greatest signals around 30% of total stride cycle.

GE

At 0.35-0.45ms^{-1} walking speeds, the M. gastrocnemius externus was active during mid-late stance, becoming active into early swing phase at faster speeds.

Our cross-correlation analysis of mean EMG timings for the GE of Crocodylia and GL of Aves showed that these were most similar for Aves, and distinct for Crocodylia (Table 7). Interestingly, the maximal correlations of timings for Crocodylia were more similar to those of Palaeognathae and quails, whereas guineafowl and turkey were most similar to each other; with pheasant values in between these. However, these similarities in maximal correlations were not so evident in the offsets of EMG timings, which were ~18-27% of a stride earlier in swing (start-signal) and stance (end-signal) for all Aves vs. Crocodylia.

Discussion

We have presented a compilation of the largest dataset of electromyographic data for archosaurs to date, including the first for emus and tinamous, thus adding palaeognathous birds to the existing literature for birds and Nile crocodiles to the published data for Crocodylia. Below, we consider our avian data first, then crocodilian EMG data, then all data in the broader context of archosaurian neuromuscular evolution.

Published hindlimb EMG data from birds to date are primarily from guineafowl (*Numida*) and domestic chickens (Jacobson and Hollyday, 1982; Gatesy, 1999; Ellerby and Marsh, 2010), as well as wild turkeys (Roberts and Gabaldón, 2008), although some important data also exist for pigeons (Gatesy and Dial, 1993, 1996). The guineafowl data presented here compare well with previously published guineafowl data, both in terms of patterns and timings for the GL and DFIV muscles; bolstering confidence in our results (Gatesy, 1999; Daley and Biewener, 2003; Gordon et al., 2015).

Prior to this study, there were no palaeognath EMG data, and the only relevant data were derived from a musculoskeletal simulation studies of emus (Goetz et al., 2008) and ostriches (Rankin et al., 2016), which predicted muscle activations for walking and running. Goetz et al. (2008) only depicted muscle forces rather than activations, and solely for the stance phase—but for 40 muscles or subdivisions thereof. Rankin et al. (2016) reported activation timings (e.g. see their figure 3 for 16 muscles) that generally match the additional palaeognath EMG data we present here, with the exception of the ITC(p) which consistently had a secondary activation during swing phase in the simulations. Whilst some small peaks were evident in our ITC data for the adult emus around foot-off at slower speeds, these are likely a result of noise, and no peaks indicative of secondary activations in mid-swing were found for running emus ($u > 1.0$) (Figure 3, S1). This discrepancy between the simulated muscle activations and EMG data was also found when compared to guineafowl data (Daley et al., 2009). Furthermore, the simulated muscle activations may be

misleading because these rely on Hill-type muscle models that presume basic relationships between neural excitation, muscle activation and force, whereas in reality these relationships may be more complex (e.g. Askew and Marsh, 1998; Perreault et al., 2003; Millard et al., 2013).

Did we observe ontogenetic variation within our emu data? Whilst variation in EMG signals through ontogeny has been found *in ovo* (e.g. Watson and Bekoff, 1990), very little research has been done on post-hatching birds (see Jacobson and Hollyday, 1982; Muir et al., 1996) as neural controls appear to establish early within embryos. However, in chukar partridges (*Alectoris chukar*) there is variation between young and adult birds in EMG patterns for pectoralis muscle EMG signals during wing-assisted incline running, with younger birds having longer periods of activation of their muscles relative to the adults (Tobalske et al., 2017). We found a similar pattern of longer activation times in younger emus' leg muscles, although the variation between the different ages was small. These similarities are in contrast to turtles. Juvenile turtles can undergo significant changes in muscle activity patterns through ontogeny, usually decreasing the number of activations for muscles during the stride cycle from two to one but sometimes profoundly changing the timing of muscle activation. For example,across the ontogeny of juveniles to adults the femorotibialis muscle's activation transitions from recovery (swing) to thrust (stance) phase in swimming (Blob et al., 2008).

The M. gastrocnemius pars lateralis (GL) has the EMG patterns that are most widely studied across avian species, and serves as a useful as a reference muscle because it retains similar anatomy (origin on the lateral distal femoral condyle and insertion on the tarsometatarsus) and locomotor function (primarily ankle extension but also knee flexion) in terrestrial gait across species. Here we found that the GL's EMG activity patterns of the palaeognathous birds were almost exactly the same as those for the neognaths during walk/run behaviours (Figure 7, Table 7). Activity began in late swing phase and continued throughout much of stance, but at faster speeds became increasingly concentrated in

early stance phase, in all birds studied to date. We suggest that across cursorial, ground birds as a whole, muscle activation patterns are likely to be conserved for morphologically and functionally similar muscles. More broadly, even GL activations during walking in the more aquatically specialized mallard duck (*Anas platyrhynchos*) are similar to the species reported here (Biewener and Corning, 2001). Thus GL muscle activation patterns appear to be generally conserved across Aves and correspond to the expected functional demands inferred from anatomical origins, insertions, joint mobility and moment arms. However, there may be differences in EMG timing of the GL during the stance phase that correlate with differences in limb posture (e.g. Gatesy and Biewener, 1991; Daley and Biewener, 2011; Gordon et al., 2015; Daley and Birn-Jeffery, 2018) and anatomical variations; or perhaps even across regions of the GL.

As in the previous study of chickens (Jacobson and Hollyday, 1982), regardless of whether the crocodiles were moving within a runway or on a treadmill, their muscle activation patterns were very similar, although the range of speeds assessed was very low, approximately at their natural walking speed ($0.1 ms^{-1}$). Previously published data for Crocodylia derive entirely from the American alligator (*Alligator mississippiensis*) and spectacled caiman (*Caiman crocodilus*) hindlimb (Gatesy, 1994, 1997; Reilly and Blob, 2003); in both cases for the Alligatoroidea lineage. Here, we provide comparable data for the Crocodyloidea lineage (and the first forelimb PEC muscle EMG for Crocodylia). The M. iliotibialis 2 (IT2) of Nile crocodiles had a relatively larger EMG signal than seen in alligators but it occurred with the same timing around mid-stance (Gatesy, 1997). Whilst no filtered signals are published for the M. gastrocnemius externus (GE), summarized timings (Reilly et al., 2005) match very well with the signals seen in the Nile crocodile data at $0.345 ms^{-1}$ presented here (Table 7), despite being from different duty factors (0.6 here vs. 0.7 in Reilly et al., (2005)).

The M. transversus perinei (TP) overlies the M. caudofemoralis longus (CFL) in Crocodylia (Romer, 1923; Frey, 1982; Cong, 1998) and has similar EMG signals in terms of patterns and timings (Gatesy, 1997). Its activity has not been measured before, to our knowledge, in Reptilia. An explanation for this similar activity may be that the TP was contracting simultaneously with the CFL. The two muscles also have muscle fibres that run perpendicular to each other (TP dorsoventrally, CFL craniocaudally). Perhaps the TP performs some function of locomotor relevance, limiting bulging of the distal CFL belly near where it narrows into its insertion, or acts similarly to the M. caudofemoralis brevis, which seems to help to change the moment arm of the CFL in lizards (Herrel et al., 2008). However, the TP is very thin and whilst not visibly implanted within the CFL, the electrodes may have been picking up "cross-talk" signals from this much larger muscle. Regardless, these novel data from Nile crocodiles have intrinsic value for understanding function of the CFL and dynamics of the tail-to-thigh region; and our EMG data are unlike those of the homologous M. caudofemoralis (pars caudalis) of birds which is only (variably) active during late stance at fast speeds (Gatesy and Dial, 1993; Gatesy, 1999).

There are no other published forelimb EMG data for Crocodylia; however, some data exist for turtles (Rivera and Blob, 2010), which may form the sister clade to archosaurs (Hedges and Poling, 1999; Field et al., 2014 but see Gauthier et al., 1988; Lyson et al., 2012), and the perhaps more distantly related Savannah monitor lizard (*Varanus exanthematicus*) (Jenkins and Goslow, 1983). The M. pectoralis data from the literature are variable, with turtles showing activity from early to late stance phase (Rivera and Blob, 2010, 2013). In contrast, in the monitor lizard, cranial portions of the PEC were active predominantly in swing phase, whilst the middle of the PEC was active at low levels during stance phase. In our Nile crocodile subject, the electrode was inserted into the cranial (i.e. major sternal) portion of the PEC, but had activity through mid-to-late stance. The differences between the species might relate to differences in the role of the pectoralis in resisting

glenohumeral abduction imposed by ground reaction forces, whether due to the “high-walking” postures in crocodiles or the added mass of the shell in turtles.

What, then, do our EMG data indicate about the evolution of muscle activity in the clade Archosauria? There are scarce overlapping and ideally comparable data, major differences in locomotor biomechanics and some issues with muscle homology (Rowe, 1986; Gatesy, 1994) that are cause for caution. On the other hand, there are clearly corresponding patterns of muscle activity that also match similarities in limb dynamics and/or muscle anatomy for Archosauria (and even other tetrapods) (Figure 9). For example, the large, ventral M. pectoralis would be expected to be an antigravity muscle from the anatomy and indeed both Crocodylia (represented by our new data for *Crocodylus niloticus*) and Aves activate M. pectoralis during their major antigravity functions (i.e. stance phase for the former; downstroke of flight for the latter) (Gatesy and Dial, 1993, 1996; Goslow et al., 2000) as expected for this large, ventrally disposed muscle. This antigravity activity is broadly shared with turtles and Squamata (*Varanus exanthematicus*: caudal PEC region), consistent with some “neuromotor conservation” at least across the broader amniote clade Sauria (Jenkins and Goslow, 1983; Schoenfuss et al., 2010; Rivera et al., 2011; Rivera and Blob, 2013). This apparent conserved activity would support the inference that quadrupedal archosaurs used their PEC muscles to support themselves during locomotion, much as their M. adductor femoris muscles countered abduction of the hindlimbs (Hutchinson and Gatesy, 2000). However, the swing phase activity of the cranial region of PEC in *Varanus* is cause for caution, as it does not follow the expectation of a ventrally located muscle acting simply as an anti-gravity adductor, and does not match the activity of the comparable region in *Crocodylus*.

Our hindlimb EMG data for Crocodylia and Aves indicate broadly similar stance phase activity for GE/GL in both groups of extant archosaurs; although unsurprising, this is nonetheless consistent

554 with a conserved antigravity function that would be expected possibly throughout Tetrapoda (e.g.
555 turtles (Schoenfuss et al., 2010), lizards (Reilly 1995, 1998), humans (Dietz et al., 1979), felids
556 (Rasmussen et al., 1978), and salamanders (FPC = medial gastrocnemius)(Ashley-Ross, 1995)). This
557 apparent conservatism also seems to apply to the digital flexors (FDL in the crocodile and DFIV in the
558 guineafowl; the latter homologous to a part of the former (Hutchinson, 2002)), which are also ankle
559 extensors (plantarflexors) with antigravity functions and thus show timings similar to those seen in
560 the GE/GL. Similarly, the IT2/ILPO (here represented by new data for *Crocodylus* and *Dromaius*) are
561 homologous muscles for Archosauria (Hutchinson, 2001) and exhibit stance phase activity (earlier in
562 stance/late in swing) in this study and related literature cited above, although our emus had an extra
563 potential burst that may be apomorphic. These data are most parsimoniously interpreted as
564 homologous muscle activity that was ancestral for Archosauria.

565

566 There was one potentially interesting difference in GE/GL timing we observed for Crocodylia vs.
567 Aves: the homologous GE/GL muscles are active only in stance phase in Crocodylia, whereas activity
568 starts in late swing phase in Aves (Table 7, Figure 7). Considering the grossly similar anatomy of
569 these muscles in extant archosaurs, published differences in knee and ankle joint kinematics suggest
570 one possible explanation: that the earlier onset of EMG activity in the avian GL is related to
571 maintaining synchronized knee flexion and ankle dorsiflexion across the swing-stance transition (e.g.
572 (Higham and Nelson, 2008)), unlike in Crocodylia where knee extension and ankle plantarflexion
573 occur from late swing to early stance phase (Gatesy, 1991, 1997; Reilly et al., 2005). This is simply
574 one reasonable speculation that deserves testing against alternatives such as plantigrade foot
575 posture in future studies, but we are unaware of it being previously proffered as an explanation.

576

577 Other EMG data for archosaurian hindlimb muscles are not feasible to compare directly within our
578 dataset. The CFL muscle surely maintained stance phase activity in early archosaurs (Gatesy, 1990).

Here, the overlying TP muscle of *Crocodylus* was sampled rather than the underlying CFL muscle, but the TP has barely been studied in the clade Sauria and deserves further analysis in the context of limb function. The ITC muscle of Aves is homologous with M. iliofemoralis of Crocodylia (Rowe, 1986). Our palaeognath EMG data strengthen the hypothesis that there was a switch from swing to stance phase activity of the ITC within the clade Dinosauromorpha, perhaps concurrent with the origin of bipedalism and increased need for hip abductor-based support (rather than adductors) during stance phase (Hutchinson and Gatesy, 2000). Likewise, the late swing and stance phase activity of the ILFB for emus and other birds, vs. mainly swing phase activity in *Alligator* (Gatesy, 1997; Reilly et al., 2005) and *Varanus* (Jayne et al., 1990), support the conclusion that this muscle added a prominent stance phase burst at some point after the divergence of the dinosauromorph/avian lineage from Archosauria, albeit apparently maintaining a swing phase burst in most birds (Gatesy, 1999). Stance phase activity of the FL in our one tinamou subject and trial, with other avian data (Gatesy, 1994, 1999), support the inference that this activity is ancestral for Aves. Then, considering similar activity of the FL in the lizard *Sceloporus* (Reilly, 1995), perhaps the FL has conserved stance phase (and perhaps late swing phase) activity across at least Sauria (like the GE/GL) (Reilly, 1998); although EMG data for the FL are lacking in Crocodylia.

While our data, and synthesis of data from the literature, suggest “conservatism” in muscle activation patterns across Archosauria, Sauria or even more broadly, an explanation for such patterns in terrestrial locomotion remains lacking. The vertebrate sensorimotor control system is plastic and adaptable to allow versatile function; yet retains similar elements of spinal central pattern generators and segmentally arranged reflexes across vertebrates (Grillner and Wallén, 1985). Hardwired neural circuitry does not require conserved activation patterns if that circuitry itself enables adaptive feedback (e.g. central pattern generators are well known to be entrained/regulated by sensory feedback and descending control). However, our data here, and

604 from other recent studies; e.g. turtles (Rivera et al., 2011; Rivera and Blob, 2013); suggest that many
605 patterns of activation broadly are conserved. One potential reason is that the shared functional
606 demands of terrestrial locomotion across all animals (e.g. supporting body weight), combined with
607 shared substrates of actuation and control (muscle and nervous system intrinsic physical properties),
608 mean that most terrestrial animals use similar mechanisms for economic movement, which is
609 reflected in conserved function in muscles that have grossly similar morphology. However, other
610 perspectives have cited reasons to be wary (Smith, 1994; Alfaro and Herrel, 2001).

611

612 Yet regardless of the cause(s) of a lack of change of motor patterns, such homology is valuable to
613 evolutionary biomechanists. Here, we have added to other perspectives on the evolution of
614 appendicular muscle control in archosaurs (Gatesy, 1990, 1999; Gatesy and Dial, 1996; Hutchinson
615 and Gatesy, 2000; Reilly et al., 2005) by showing how a forelimb muscle (PEC) and several hindlimb
616 muscles (IT2/ILPO, ILFB, GE/GL, FDL/DFIV, potentially FL) have maintained similar motor patterns in
617 extant Archosauria, although the avian GL has modified its timing (Figure 9). These similarities were
618 somewhat expected from relatively conservative muscle morphology, and supported prior studies
619 (Gatesy, 1994, 1999), yet the GL timing difference might be less expected. This overall similarity of
620 muscle activations bolsters their usage in validating computer simulations, or otherwise inferring
621 locomotor function, for taxa without available EMG data, whether they are extant archosaurs (Goetz
622 et al., 2008; Rankin et al., 2016) or extinct, as long as the muscles are known or can be inferred
623 (Witmer, 1995). However, the evidence for changes of (or additions to) the motor patterns of avian
624 muscles such as the morphologically transformed ITC and more morphologically conservative ILFB is
625 cause for caution (neuromotor conservation demands to be tested, not assumed (Gatesy, 1994,
626 1999; Smith, 1994; Goslow et al., 2000; Rivera et al., 2011; Rivera and Blob, 2013)), and cause for
627 assembling datasets from more varied taxa and behaviours.

628

Contributions

JRH and MAD conceived the study. ARC, VRA, KBM, LPL and MAD all planned and performed surgeries on the animals, assisted by CA, PM and LP. ARC, VRA, KBM, LPL, MAD and JRH all carried out experiments. ARC conducted the data analysis assisted by MAD. ARC wrote the manuscript aided by JRH and MAD. All authors contributed to reviewing the manuscript and approved the final draft.

Acknowledgements

Enrico Eberhard, Peter Bishop and Jorn Cheney all provided advice on Matlab code. We thank La Ferme aux Crocodiles (Pierrelatte, France) for provision of the Nile crocodile subjects. We appreciate the support of the Biological Services Unit at RVC for animal care. We thank Russell Main, Emily Sparkes, Sandra Shefelbine and Heather Paxton for help with the experimental data collection for emus, and Jeffery Rankin and James Usherwood for input on that study. Thanks to Alison Tarbell and Sheridan Golding for assistance in quail, turkey and pheasant data collection. This study was supported by funding from The Royal Veterinary College and the European Research Council (ERC) under the European Union's Horizon 2020 research and innovation programme (grant agreement #695517). Finally thanks to the anonymous reviewers whose comments greatly improved the manuscript.

Conflict of Interests

None are declared.

References

Alexander RM, Jayes AS. 1983. A dynamic similarity hypothesis for the gaits of quadrupedal mammals. J Zool 201:135–152.

652 Alfaro ME, Herrel A. 2001. Introduction: major issues of feeding motor control in vertebrates. Am
653 Zool 41:1243–1247.

654 Allen V, Molnar J, Parker W, Pollard A, Nolan G, Hutchinson JR. 2014. Comparative architectural
655 properties of limb muscles in Crocodylidae and Alligatoridae and their relevance to divergent
656 use of asymmetrical gaits in extant Crocodylia. J Anat 225:569–582.

657 Altimiras J, Lindgren I, Giraldo-Deck LM, Matthei A, Garitano-Zavala Á. 2017. Aerobic performance in
658 tinamous is limited by their small heart. A novel hypothesis in the evolution of avian flight.
659 Sci Rep 7:15964.

660 Ashley-Ross MA. 1995. Patterns of hind limb motor output during walking in the salamander
661 *Dicamptodon tenebrosus*, with comparisons to other tetrapods. J Comp Physiol A 177: 273-
662 285.

663 Askew GN, Marsh RL. 1998. Optimal shortening velocity (V/Vmax) of skeletal muscle during cyclical
664 contractions: length-force effects and velocity-dependent activation and deactivation. J Exp
665 Biol 201:1527–1540.

666 Bekoff A. 1976. Ontogeny of leg motor output in the chick embryo: a neural analysis. Brain Res
667 106:271–291.

668 Bekoff A, Nusbaum MP, Sabichi AL, Clifford M. 1987. Neural control of limb coordination. I.
669 Comparison of hatching and walking motor output patterns in normal and deafferented
670 chicks. J Neurosci 7:2320–2330.

671 Blob RW, Rivera ARV, Westneat MW. 2008. Hindlimb Function in Turtle Locomotion: Limb
672 Movements and Muscular Activation across Taxa, Environment, and Ontogeny. In: Wyneken
673 J, Godfrey MH, Bels V, editors. *Biology of Turtles*. Boca Raton, FL: CRC Press. p. 139–162.

674 Bradley NS, Bekoff A. 1992. Development of coordinated movement in chicks: II. Temporal analysis
675 of hindlimb muscle synergies at embryonic day 10 in embryos with spinal gap transections. J
676 Neurobiol 23:420–432.

677 Bradley NS, Ryu YU, Yeseta MC. 2014. Spontaneous locomotor activity in late-stage chicken embryos
678 is modified by stretch of leg muscles. J Exp Biol 217:896–907.

679 Carr JA, Ellerby DJ, Marsh RL. 2011. Function of a large biarticular hip and knee extensor during
680 walking and running in guinea fowl (*Numida meleagris*). J Exp Biol 214:3405–3413.

681 Cong L. 1998. *Yangzi e da ti jie pou = The gross anatomy of* Alligator sinensis *(Fauvel)*. Di 1 ban. ed.
682 Beijing: Ke xue chu ban she.

683 Daley MA, Biewener AA. 2003. Muscle force-length dynamics during level versus incline locomotion:
684 a comparison of in vivo performance of two guinea fowl ankle extensors. J Exp Biol
685 206:2941–2958.

686 Daley MA, Biewener AA. 2011. Leg muscles that mediate stability: mechanics and control of two
687 distal extensor muscles during obstacle negotiation in the guinea fowl. Philos Trans R Soc
688 Lond B, Biol Sci 366:1580–1591.

689 Daley MA, Birn-Jeffery A. 2018. Scaling of avian bipedal locomotion reveals independent effects of
690 body mass and leg posture on gait. J Exp Biol 221.

691 Daley MA, Voloshina A, Biewener AA. 2009. The role of intrinsic muscle mechanics in the
692 neuromuscular control of stable running in the guinea fowl. J Physiol (Lond) 587:2693–2707.

693 Dietz V, Schmidtbleicher D, Noth J. 1979. Neuronal mechanisms of human locomotion. J
694 Neurophysiol 42:1212–1222.

695 Ellerby DJ, Marsh RL. 2010. The mechanical function of linked muscles in the guinea fowl hind limb. J
696 Exp Biol 213:2201–2208.

697 Field DJ, Gauthier JA, King BL, Pisani D, Lyson TR, Peterson KJ. 2014. Toward consilience in reptile
698 phylogeny: miRNAs support an archosaur, not lepidosaur, affinity for turtles. Evol Dev
699 16:189–196.

700 Foster KL, Higham TE. 2014. Context-dependent changes in motor control and kinematics during
701 locomotion: modulation and decoupling. Proc Biol Sci 281:20133331.

702 Foster KL, Higham TE. 2017. Integrating gastrocnemius force-length properties, in vivo activation and
703 operating lengths reveals how *Anolis* deal with ecological challenges. J Exp Biol 220:796–806.

704 Frey E. 1982. Ecology, locomotion and tail muscle anatomy of crocodiles. Neues Jahrbuch fur
705 Geologie und Paläontologie - Abhandlungen 164:194–199.

706 Gatesy SM. 1990. Caudefemoral musculature and the evolution of theropod locomotion.
707 Paleobiology 16:170–186.

708 Gatesy SM. 1991. Hind limb movements of the American alligator (*Alligator mississippiensis*) and
709 postural grades. J Zool 224:577–588.

710 Gatesy SM. 1994. Neuromuscular diversity in archosaur deep dorsal thigh muscles. Brain Behav Evol
711 43:1–14.

712 Gatesy SM. 1997. An electromyographic analysis of hindlimb function in *Alligator* during terrestrial
713 locomotion. J Morphol 234:197–212.

714 Gatesy SM. 1999. Guineafowl hind limb function. II: Electromyographic analysis and motor pattern
715 evolution. J Morphol 240:127-142.

716 Gatesy SM, Biewener AA. 1991. Bipedal locomotion: effects of speed, size and limb posture in birds
717 and humans. J Zool 224:127–147.

718 Gatesy SM, Dial KP. 1993. Tail muscle activity patterns in walking and flying pigeons (*Columba livia*). J
719 Exp Biol 176:55-76..

720 Gatesy SM, Dial KP. 1996. From frond to fan: *Archaeopteryx* and the evolution of short-tailed birds.
721 Evolution 50:2037-2048.

722 Gauthier J, Kluge AG, Rowe T. 1988. Amniote phylogeny and the importance of fossils. Cladistics
723 4:105–209.

724 Goetz JE, Derrick TR, Pedersen DR, Robinson DA, Conzemius MG, Baer TE, Brown TD. 2008. Hip joint
725 contact force in the emu (*Dromaius novaehollandiae*) during normal level walking. J Biomech
726 41:770–778.

727 Gordon JC, Rankin JW, Daley MA. 2015. How do treadmill speed and terrain visibility influence
728 neuromuscular control of guinea fowl locomotion? J Exp Biol 218:3010–3022.

729 Goslow GE, Wilson D, Poore SO. 2000. Neuromuscular correlates to the evolution of flapping flight in
730 birds. Brain Behav Evol 55:85–99.

731 Grillner S, Wallén P. 1985. Central pattern generators for locomotion, with special reference to
732 vertebrates. Annu Rev Neurosci 8:233–261.

733 Hedges SB, Poling LL. 1999. A molecular phylogeny of reptiles. Science 283:998–1001.

734 Herrel A, Vanhooydonck B, Porck J, Irschick DJ. 2008. Anatomical basis of differences in locomotor
735 behavior in anolis lizards: A comparison between two ecomorphs. Bull Mus Comp Zool
736 159:213–238.

737 Higham TE, Biewener AA, Wakeling JM. 2008. Functional diversification within and between muscle
738 synergists during locomotion. Biol Lett 4:41–44.

739 Higham TE, Jayne BC. 2004. In vivo muscle activity in the hindlimb of the arboreal lizard, *Chamaeleo*
740 *calyptratus*: general patterns and the effects of incline. J Exp Biol 207:249–261.

741 Higham TE, Nelson FE. 2008. The integration of lateral gastrocnemius muscle function and
742 kinematics in running turkeys. Zoology (Jena) 111:483–493.

743 Hudson GE, Schreiweis DO, Wang SYC, Lancaster DA. 1972. A numerical study of the wing and leg
744 muscles of tinamous Tinamidae. Northwest Science 46:207-255.

745 Hutchinson J. 2001. The evolution of pelvic osteology and soft tissues on the line to extant birds
746 (Neornithes). Zool J Linn Soc 131:123–168.

747 Hutchinson JR. 2002. The evolution of hindlimb tendons and muscles on the line to crown-group
748 birds. Comp Biochem Physiol Part A, Mol Integr Physiol 133:1051–1086.

749 Hutchinson JR, Gatesy SM. 2000. Adductors, abductors, and the evolution of archosaur locomotion.
750 Paleobiology 26:734–751.

751 Jacobson RD, Hollyday M. 1982. A behavioral and electromyographic study of walking in the chick. J
752 Neurophysiol 48:238–256.

753 Jayne BC, Bennett AF, Lauder GV. 1990. Muscle recruitment during terrestrial locomotion: How
754 speed and temperature affect fibre type use in a lizard. J Exp Biol.

755 Jenkins FA, Goslow GE. 1983. The functional anatomy of the shoulder of the savannah monitor lizard
756 (*Varanus exanthematicus*). J Morphol 175:195–216.

757 Lamas LP, Main RP, Hutchinson JR. 2014. Ontogenetic scaling patterns and functional anatomy of the
758 pelvic limb musculature in emus (*Dromaius novaehollandiae*). PeerJ 2:e716.

759 Lamas LRGP. 2015. Musculoskeletal biomechanics during growth on emu (*Dromaius*; Aves): an
760 integrative experimental and modelling analysis [Doctoral dissertation]. Royal Veterinary
761 College, United Kingdom.

762 Lyson TR, Sperling EA, Heimberg AM, Gauthier JA, King BL, Peterson KJ. 2012. MicroRNAs support a
763 turtle + lizard clade. Biol Lett 8:104–107.

764 Marsh RL, Ellerby DJ, Carr JA, Henry HT, Buchanan CI. 2004. Partitioning the energetics of walking
765 and running: swinging the limbs is expensive. Science 303:80–83.

766 Meers MB. 2003. Crocodylian forelimb musculature and its relevance to Archosauria. Anat Rec A
767 Discov Mol Cell Evol Biol 274:891–916.

768 Millard M, Uchida T, Seth A, Delp SL. 2013. Flexing computational muscle: modeling and simulation
769 of musculotendon dynamics. J Biomech Eng 135:021005.

770 Monticelli P, Ronaldson HL, Hutchinson JR, Cuff AR, d Ovidio D, Adami C. 2019. Medetomidine-
771 ketamine-sevoflurane anaesthesia in juvenile Nile crocodiles (*Crocodylus niloticus*)
772 undergoing experimental surgery. Vet Anaesth Analg 46:84-89.

773 Muir GD, Gosline JM, Steeves JD. 1996. Ontogeny of bipedal locomotion: walking and running in the
774 chick. J Physiol (Lond) 493:589–601.

775 Perreault EJ, Heckman CJ, Sandercock TG. 2003. Hill muscle model errors during movement are
776 greatest within the physiologically relevant range of motor unit firing rates. J Biomech
777 36:211–218.

778 Prum RO, Berv JS, Dornburg A, Field DJ, Townsend JP, Lemmon EM, Lemmon AR. 2015. A
779 comprehensive phylogeny of birds (Aves) using targeted next-generation DNA sequencing.
780 Nature 526:569–573.

781 Rankin JW, Rubenson J, Hutchinson JR. 2016. Inferring muscle functional roles of the ostrich pelvic
782 limb during walking and running using computer optimization. J R Soc Interface
783 13:20160035.

784 Rasmussen S, Chan AK, Goslow GE. 1978. The cat step cycle: electromyographic patterns for
785 hindlimb muscles during posture and unrestrained locomotion. J Morphol 155:253–269.

786 Reilly SM. 1995. Quantitative electromyography and muscle function of the hind limb during
787 quadrupedal running in the lizard *Sceloporus clarki*. Zoology 98:263–263.

788 Reilly SM. 1998. Sprawling locomotion in the lizard *Sceloporus clarkii*: speed modulation of motor
789 patterns in a walking trot. Brain Behav Evol 52:126–138.

790 Reilly SM, Blob RW. 2003. Motor control of locomotor hindlimb posture in the American alligator
791 (*Alligator mississippiensis*). J Exp Biol 206:4327–4340.

792 Reilly SM, Willey JS, Biknevicius AR, Blob RW. 2005. Hindlimb function in the alligator: integrating
793 movements, motor patterns, ground reaction forces and bone strain of terrestrial
794 locomotion. J Exp Biol 208:993–1009.

795 Rivera ARV, Blob RW. 2010. Forelimb kinematics and motor patterns of the slider turtle (*Trachemys*
796 *scripta*) during swimming and walking: shared and novel strategies for meeting locomotor
797 demands of water and land. J Exp Biol 213:3515–3526.

798 Rivera ARV, Blob RW. 2013. Forelimb muscle function in pig-nosed turtles, *Carettochelys insculpta*:
799 testing neuromotor conservation between rowing and flapping in swimming turtles. Biol Lett
800 9:20130471.

801 Rivera ARV, Wyneken J, Blob RW. 2011. Forelimb kinematics and motor patterns of swimming
802 loggerhead sea turtles (*Caretta caretta*): are motor patterns conserved in the evolution of
803 new locomotor strategies? J Exp Biol 214:3314–3323.

Roberts TJ, Gabaldón AM. 2008. Interpreting muscle function from EMG: lessons learned from direct measurements of muscle force. Integr Comp Biol 48:312–320.

Romer AS. 1923. Crocodilian pelvic muscles and their avian and reptilian homologues. Bulletin of the AMNH 48(15).

Rowe T. 1986. Homology and evolution of the deep dorsal thigh musculature in birds and other reptilia. J Morphol 189:327–346.

Schoenfuss HL, Roos JD, Rivera ARV, Blob RW. 2010. Motor patterns of distal hind limb muscles in walking turtles: Implications for models of limb bone loading. J Morphol 271:1527–1536.

Smith KK. 1994. Are neuromotor systems conserved in evolution? Brain Behav Evol 43:293–305.

Tobalske BW, Jackson BE, Dial KP. 2017. Ontogeny of fight capacity and pectoralis function in a precocial ground bird (*Alectoris chukar*). Integr Comp Biol 57:217–230.

Vanden Berge JC, Zweers GA. 1993. Myologia. In: Baumel JJ, King AS, Breazile JE, Evans HE, Vanden Berge JC, editors. *Handbook of Avian Anatomy: Nomina Anatomica Avium*. Cambridge, Massachusetts, USA: Nuttal Ornithological Club.

Witmer LM. 1995. The extant phylogenetic bracket and the importance of reconstructing soft tissues in fossils. In: Thomason JJ, editor. F*unctional Morphology in Vertebrate Paleontology.* New York: Cambridge University Press. p. 19–33.

Yonezawa T, Segawa T, Mori H, Campos PF, Hongoh Y, Endo H, Akiyoshi A, Kohno N, Nishida S, Wu J, Jin H, Adachi J, Kishino H, Kurokawa K, Nogi Y, Tanabe H, Mukoyama H, Yoshida K, Rasoamiaramanana A, Yamagishi S, Hayashi Y, Yoshida A, Koike H, Akishinonomiya F, Willerslev E, Hasegawa M. 2017. Phylogenomics and morphology of extinct paleognaths reveal the origin and evolution of the ratites. Curr Biol 27:68–77.

Figure 1. Avian and crocodile muscles from which EMG data were obtained . A) Avian hindlimb is from a representative tinamou; figure modified from (Hudson et al., 1972). Muscle abbreviations from Table 2. B) Crocodile hindlimb dorsal view, C) crocodile forelimb ventral view. Both right limbs, modified from Allen et al., (2014). Muscle abbreviations in Table 3.

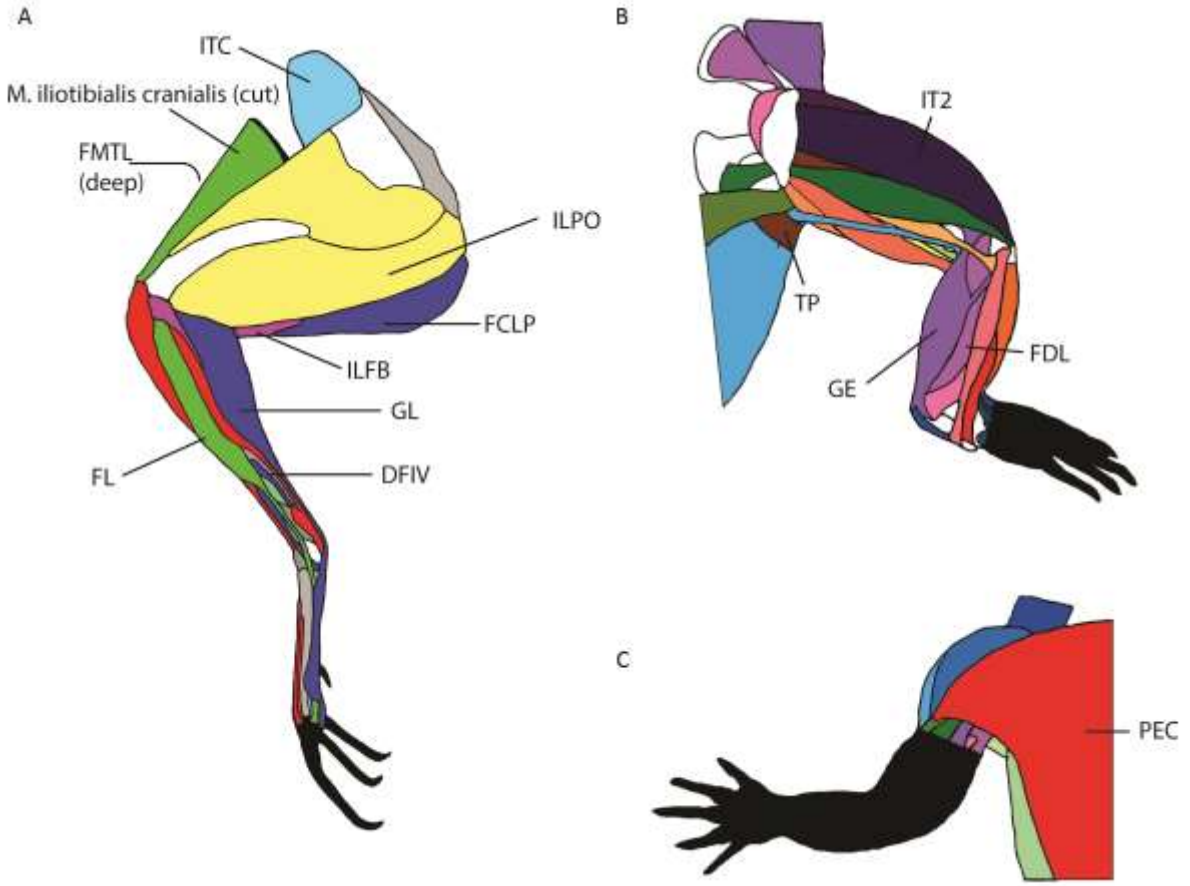

834 Figure 2. Filtered EMG signals from three emus at three ages, showing the signal variation at 1.1-1.3
835 dimensionless speed.

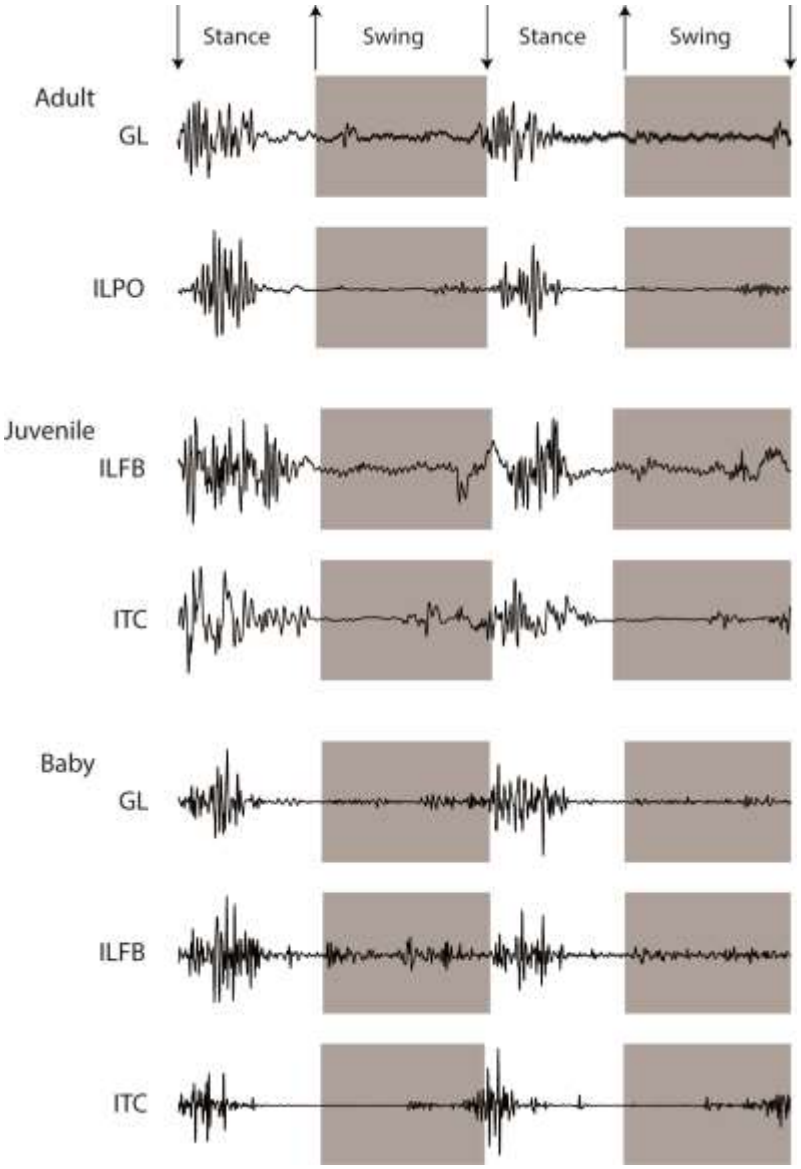

836

837

838 Figure 3. Timing of emu muscle activations at 1.1-1.3 dimensionless speed. Bars represent average
839 periods of activity, with the lines representing 95% confidence intervals. Vertical dashed lines are
840 foot-off events.

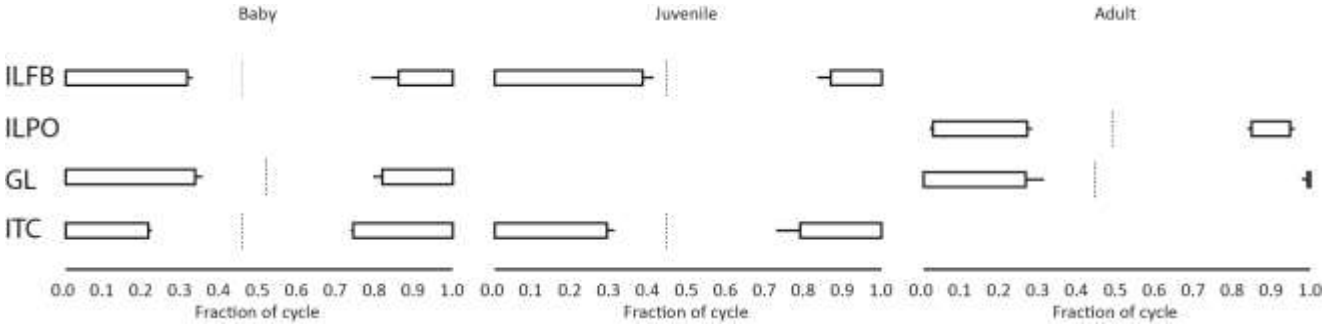

841

842

843 Figure 4. Timing of tinamou muscle activations for A-C) GL, and D) FL muscles. A,D) *u* = 0.06, B) *u* =
844 0.23, C) *u* = 0.29. Bars represent average period of activity, with the lines representing 95%
845 confidence intervals. Vertical dashed lines are foot-off events.

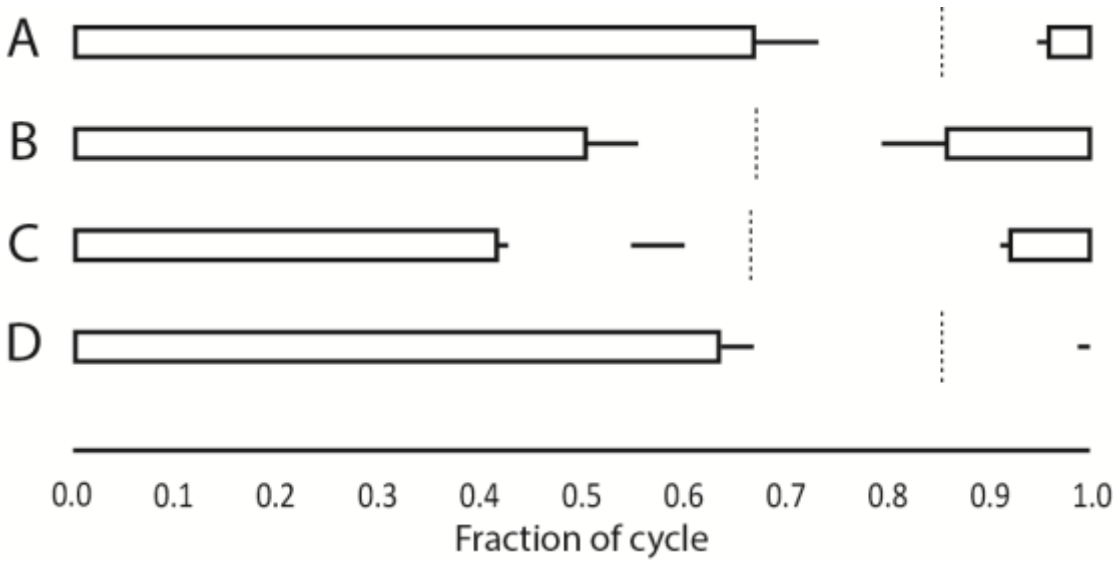

846

847

Figure 5. Turkey muscle activation timing at 1.2 dimensionless speed for FCLP, GL and DFIV muscles. Bars represent average period of activation, with the lines representing 95% confidence intervals. Vertical dashed lines are foot-off events.

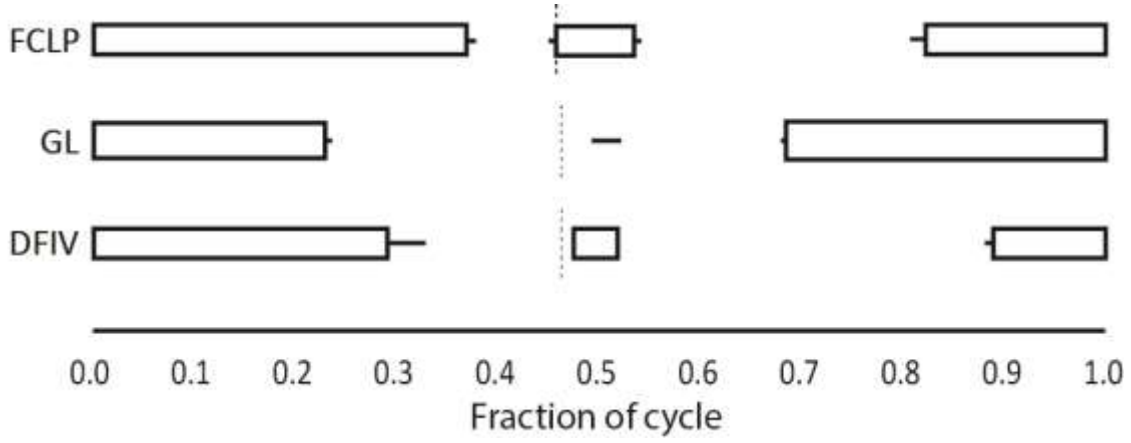

Figure 6. Timing of guineafowl muscle activity at 1.2 dimensionless speed for FMTL, GL and DFIV muscles. Bars represent average activations, with the lines representing 95% confidence intervals. Vertical dashed lines are foot-off events.

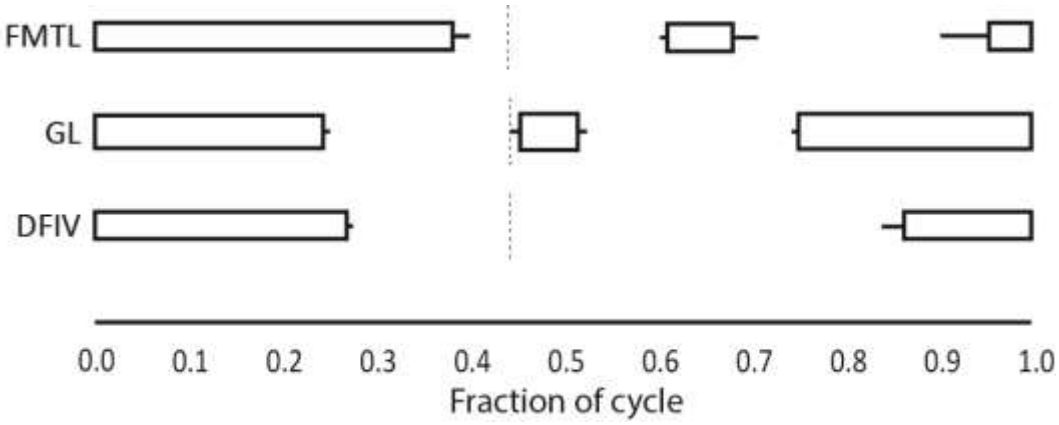

Figure 7. Activation timing for M. gastrocnemius pars lateralis (GL) across bird species at similar dimensionless speed (1.1-1.3*u*). A) turkey, B) guineafowl, C) pheasant, D) quail, E) emu, F) tinamou (0.29*u*). Bars represent average period of activation, with the lines representing 95% confidence intervals. Vertical dashed lines are foot-off events.

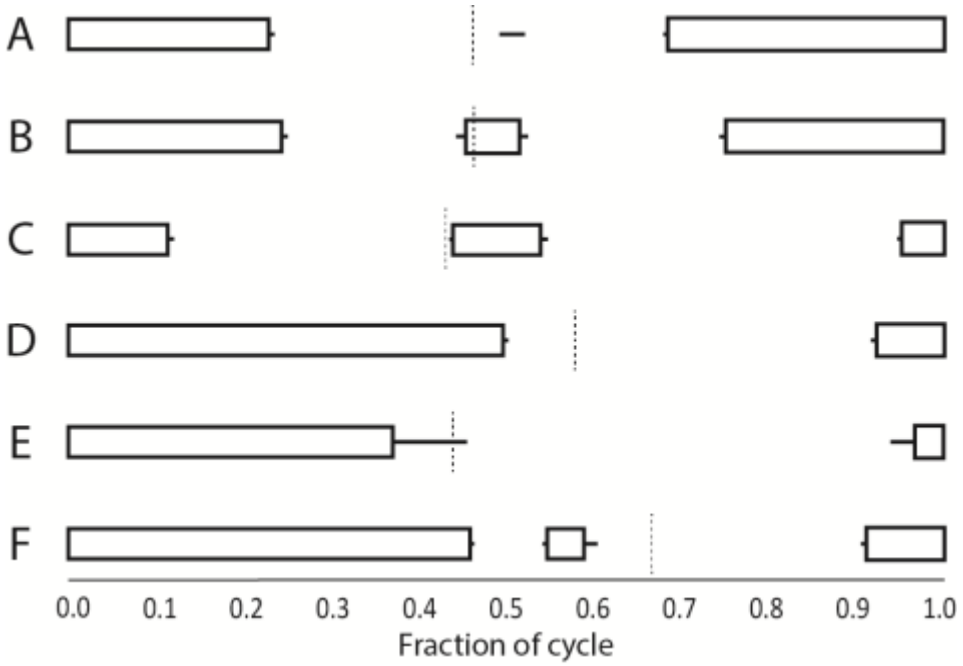

Figure 8. Timing of crocodile muscle activity. Bars represent average activations, with the lines representing 95% confidence intervals. Vertical dashed lines are foot-off events.

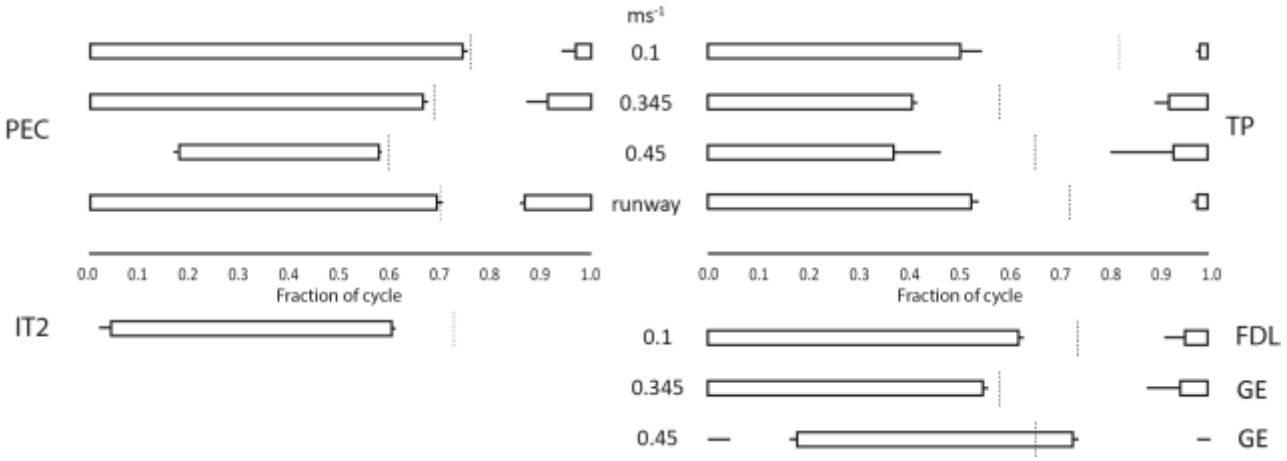

Figure 9. Phylogeny of Sauria (based on Gauthier et al., 1988; Hedges and Poling, 1999; Field et al., 2014; Prum et al., 2015), with the most parsimonious reconstruction of the evolution of EMG patterns mapped onto it (following Gatesy 1994, 1999). Muscle abbreviations are in Tables 2 and 3. "?" for turtle stem reflects controversy over their precise phylogenetic position. Nodes for Sauria, Archosauria and Aves are annotated with key ancestral EMG patterns for muscles focused on in this study; simplified into "Stance" (circle filled on right half) for mainly stance phase activity (potentially with some late swing phase), "Swing" (circle filled on left half) for mainly swing phase activity, and a "Stance" circle rotated 30 degrees anticlockwise for the more pronounced earlier swing phase activity (and earlier stance phase end of activity) evident in the GL of Aves. Additional EMG data for ducks (Biewener and Corning, 2001) and pigeons (Gatesy and Dial, 1993, 1996) further bolster the results here for Aves but for simplicity are not shown.

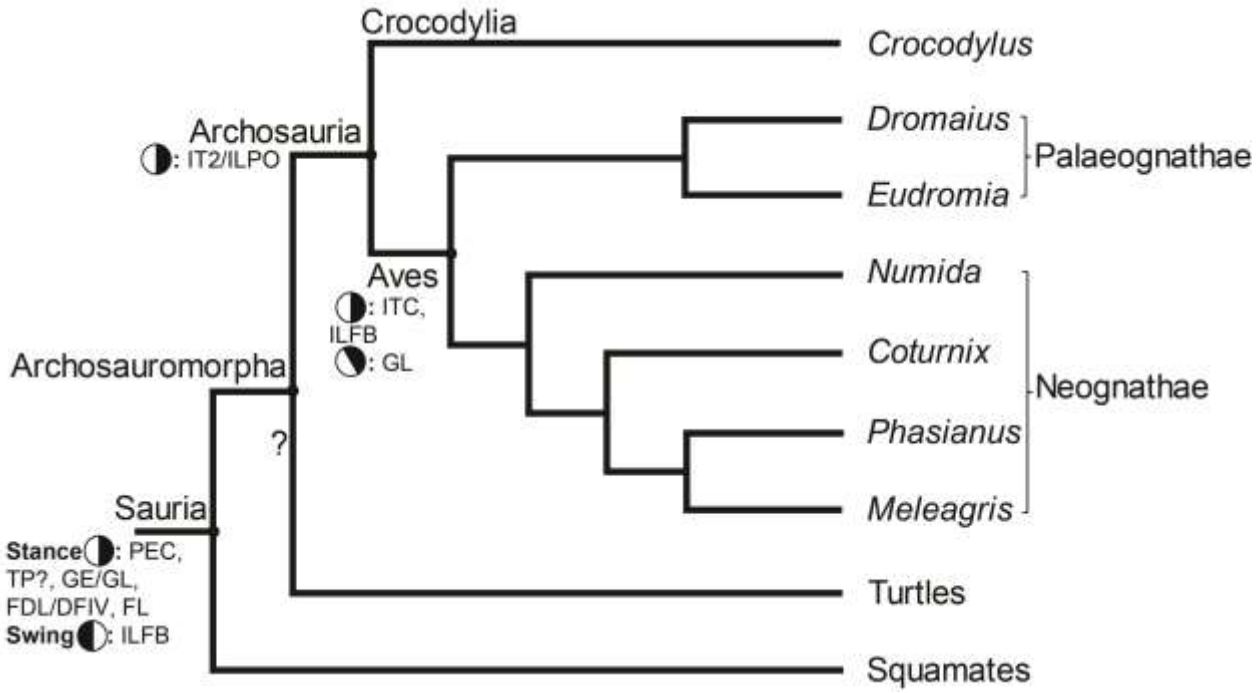

Table 1. Species used in the study

Species	Common name	Ontogenetic stage	Number of individuals	Sex	Mass (kg)
Crocodylus niloticus	Nile crocodile	Juvenile	4	F	1.59-4.63
Dromaius novaehollandiae	Emu	Baby, Juvenile, Adult	2 2 2	Unknown	3.95-4.1, 17-18, 36-37
Eudromia elegans	Elegant-crested tinamou	Adult	2	F,M	0.555-0.616
Numida meleagris	Guineafowl	Adult	2	F,M	1.5, 1.7
Phasianus colchicus	Common pheasant	Adult	2	M	1.0, 1.1
Coturnix virginianus	Bobwhite quail	Adult	2	F	0.15, 0.17
Meleagris gallopavo	Wild turkey	Adult	2	F	5.2, 6.0

Table 2. Bird muscles that EMG data were obtained from, with previously reported anatomy and function. Nomenclature follows Vanden Berge and Zweers (1993) for Aves. “Actions” (presumed potential functions around joints crossed) are inferred from anatomy following Vanden Berge and Zweers (1993) and Lamas et al. (2014).

Muscle	Origin	Insertion	Action
Iliotrochantericus caudalis (ITC)	Preacetabular ilium	Trochanteric crest of proximal femur	Hip flexor, abductor and internal rotator
Iliotibialis lateralis pars postacetabularis (ILPO)	Dorsal postacetabular ilium	Patella and cranial tibial crest of tibiotarsus	Hip extensor, abductor and external rotator; knee extensor
Iliofibularis (ILFB)	Postacetabular ilium	Fibula (M. iliofibularis tubercle)	Hip extensor, abductor and external rotator; knee flexor
Flexor cruris lateralis pars pelvica (FCLP)	Posterior rim of terminal iliac process	GE/GL and flexor cruris medialis tendon	Hip extensor, abductor and external rotator; knee flexor
Femorotibialis lateralis (FMTL)	Lateral surface of femur	Craniolateral surface of proximal tibiotarsus	Knee extensor
Gastrocnemius pars lateralis (GL)	Caudal side of lateral condyle of femur	Caudal surface of proximal (tarso)metatarsus (i.e. hypotarsus of birds)	Knee flexor; ankle extensor
Fibularis longus (FL)	Craniolateral surface of proximal tibiotarsus	Tarsus (with connections to digital flexor tendons)	Ankle extensor (and potentially digital flexor)
Flexor perforatus digiti IV (DFIV)	Lateral knee ligaments	Phalanx IV of Digit IV	Ankle extensor; digit IV flexor

Table 3. Crocodile muscles that EMG data were obtained from, with previously reported anatomy and function. Nomenclature follows Meers (2003) and Allen et al. (2014) and references therein for Crocodylia. “Actions” (presumed potential functions around joints crossed) are inferred from anatomy.

Muscle	Origin	Insertion	Action
Pectoralis (PEC)	Ventral surface of sternum, ribcage, surrounding area	Deltopectoral crest of humerus	Glenohumeral extensor, abductor and supinator
Transversus perinei (TP)	Ischium	Centra of caudal vertebrae 1+2	Unknown: possibly shaping tail base
Iliotibialis 2 (IT2)	Dorsal ilium	Cranial side of proximal tibia	Hip abductor (also long-axis rotator and flexor/extensor?); knee extensor
Gastrocnemius externus (GE)	Caudal side of lateral condyle of femur	Caudal surface of proximal (tarso)metatarsus	Knee flexor; ankle extensor
Flexor digitorum longus – hindlimb (FDL)	Disto-lateral femoral condyle	Distal pes	Digital flexor; ankle extensor

Table 4. EMG data summary for bird subjects.

Species	Tinamou				Turkey			Pheasant	Quail	Guineafowl		
Muscle	GL			FL	GL	FCLP	DFIV	GL	GL	GL	DFIV	FMTL
N individuals	1	1	1	1	2	2	2	1	2	2	2	2
Surface	Treadmill	Treadmill	Treadmill	Treadmill	Treadmill	Treadmill	Treadmill	Treadmill	Treadmill	Treadmill	Treadmill	Treadmill
Speed (ms^{-1})	0.10	0.35	0.45	0.10	2.15	2.15	2.15	1.7	1.12	1.7	1.7	1.7
u	0.06	0.23	0.29	0.06	1.27	1.27	1.27	1.25	1.23	1.28	1.28	1.28
# trials	2	2	2	2	5	5	5	1	6	6	6	6
# steps	7	7	17	7	46	46	46	14	45	54	54	54

Table 5. EMG trial and data summary for Nile crocodile subjects.

Species	Nile crocodile											
Muscle	TP				IT2	FDL	PEC				GL	
N individuals	1	2	1	1	1	1	1	1	1	1	1	1
Surface	Runway	Treadmill	Treadmill	Treadmill	Treadmill	Treadmill	Runway	Treadmill	Treadmill	Treadmill	Treadmill	Treadmill
Speed (ms^{-1})	0.10	0.10	0.35	0.45	0.10	0.10	0.10	0.10	0.35	0.45	0.35	0.45
u	0.07	0.07	0.26	0.33	0.07	0.07	0.07	0.07	0.26	0.33	0.26	0.33
# trials	5	9	2	2	2	5	5	4	2	2	2	2
# steps	14	25	8	7	6	16	14	19	8	9	8	7

Table 6. EMG trial and data summary for emu subjects across ontogeny.

	Emu - adult									
Muscle	GL					ILPO				
N individuals	1	1	2	2	2	1	1	1	1	1
Surface	Runway	Runway	Runway	Runway	Runway	Runway	Runway	Runway	Runway	Runway
Speed (ms^{-1})	0.98-1.4	1.4-2.02	2.02-2.65	2.65-3.23	3.23-3.7	0.98-1.4	1.4-2.02	2.02-2.65	2.65-3.23	3.23-3.7
u	0.3-0.5	0.5-0.7	0.7-0.9	0.9-1.1	1.1-1.3	0.3-0.5	0.5-0.7	0.7-0.9	0.9-1.1	1.1-1.3
# trials	2	4	12	21	7	2	4	6	8	3
# steps	4	8	24	41	13	4	8	12	16	6

	Emu - juvenile							
Muscle	ILFB		ITC					
N individuals	1	1	1	1	1	1	1	1
Surface	Runway	Runway	Runway	Runway	Runway	Runway	Runway	Runway
Speed (ms^{-1})	2.9-3.3	3.3-4.0	1.19-1.3	1.4-1.9	1.9-2.4	2.4-2.9	2.9-3.3	3.3-4.0
u	1.1-1.3	1.3-1.5	0.3-0.5	0.5-0.7	0.7-0.9	0.9-1.1	1.1-1.3	1.3-1.5
# trials	10	9	2	1	5	7	10	9
# steps	18	16	4	2	11	15	18	16

	Emu - baby															
Muscle	GL						ILFB				ITC					
N individuals	1	1	2	1	2	2	1	1	1	1	1	1	2	1	1	1
Surface	Runway	Runway	Runway	Runway	Runway	Runway	Runway	Runway	Runway	Runway	Runway	Runway	Runway	Runway	Runway	Runway
Speed (ms^{-1})	0.6-0.92	0.92-1.3	1.3-1.7	1.7-2.0	2.0-2.4	2.4-2.7	1.3-1.7	1.7-2.0	2.0-2.4	2.4-2.7	0.6-0.92	0.92-1.3	1.3-1.7	1.7-2.0	2.0-2.4	2.4-2.7
u	0.3-0.5	0.5-0.7	0.7-0.9	0.9-1.1	1.1-1.3	1.3-1.5	0.7-0.9	0.9-1.1	1.1-1.3	1.3-1.5	0.3-0.5	0.5-0.7	0.7-0.9	0.9-1.1	1.1-1.3	1.3-1.5
# trials	2	3	11	8	19	10	7	8	9	1	2	1	9	2	10	9
# steps	6	10	43	34	81	43	26	34	40	4	6	3	31	9	41	39

Table 7. Cross-correlation analysis results for lateral gastrocnemius (GL/GE) EMG timings for all species at 1.1-1.3*u* or maximal speed obtained. “Max Cor” is the maximum correlation between the average signals; “offset” is the offset of the maximum correlations between the species (as fraction of a stride). “Croc” is Nile crocodile; “Guinea” is guineafowl.

	Croc	Emu	Quail	Tinamou	Turkey	Guinea	Pheasant	
Croc	1.000	0.855	0.802	0.817	0.487	0.478	0.746	Max Cor
	0.000	0.178	0.230	0.228	0.266	0.230	0.183	Offset
Emu		1.000	0.940	0.941	0.728	0.699	0.834	Max Cor
		0.000	0.000	0.000	0.014	0.020	0.000	Offset
Quail			1.000	0.953	0.814	0.789	0.900	Max Cor
			0.000	0.000	0.004	0.012	0.000	Offset
Tinamou				1.000	0.759	0.753	0.869	Max Cor
				0.000	0.000	0.000	0.000	Offset
Turkey					1.000	0.970	0.788	Max Cor
					0.000	0.000	0.000	Offset
Guinea						1.000	0.782	Max Cor
						0.000	0.000	Offset